JCIM JOURNAL OF CHEMICAL INFORMATION AND MODELING

pubs.acs.org/jcim Article

Incorporating Target-Specific Pharmacophoric Information into Deep Generative Models for Fragment Elaboration

Thomas E. Hadfield, Fergus Imrie, Andy Merritt, Kristian Birchall, and Charlotte M. Deane*

Cite This: J. Chem. Inf. Model. 2022, 62, 2280−2292 Read Online

ACCESS | Metrics & More | Article Recommendations | Supporting Information

ABSTRACT: Despite recent interest in deep generative models for scaffold elaboration, their applicability to fragment-to-lead campaigns has so far been limited. This is primarily due to their inability to account for local protein structure or a user's design hypothesis. We propose a novel method for fragment elaboration, STRIFE, that overcomes these issues. STRIFE takes as input fragment hotspot maps (FHMs) extracted from a protein target and processes them to provide meaningful and interpretable structural information to its generative model, which in turn is able to rapidly generate elaborations with complementary pharmacophores to the protein. In a large-scale evaluation, STRIFE outperforms existing, structure-unaware, fragment elaboration methods in proposing highly ligand-efficient elaborations. In addition to automatically extracting pharmacophoric information from a protein target's FHM, STRIFE optionally allows the user to specify their own design hypotheses.

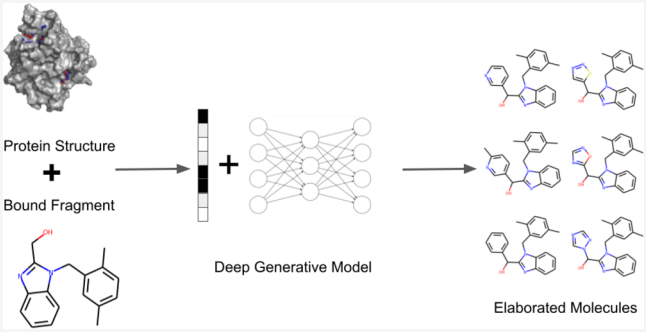

INTRODUCTION

Fragment-based drug discovery (FBDD) approaches are increasingly being used for the rational design of novel compounds.[1,2] FBDD campaigns aim to identify smaller-than-druglike molecules which bind weakly to the target and use them as a basis for developing a high-affinity binder. Compared to traditional design methodologies, FBDD methods have a number of advantages. First, starting from small fragments with low molecular weight allows a greater degree of control over the physical properties of the resulting molecule than using a druglike small molecule as a starting point.[3] They also facilitate a more efficient exploration of chemical space, with a 2005 study[4] reporting that hit rates for fragment libraries were 10−1000 times higher than standard high-throughput screening assays. Fragment-based approaches therefore offer a higher chance of identifying a starting point and enhanced control over the subsequent optimization process.

Following the identification of a set of fragment hits against a target from a fragment screen, there are three main strategies for developing a lead molecule with high binding affinity:[5] The first, elaboration (or growing), involves selecting a single fragment and adding functional groups to form further favorable interactions with the protein. The second, fragment linking, takes two fragments bound concurrently in the same region of the protein and designs a molecular bridge between them such that the resulting molecule contains both fragments as substructures. Finally, fragment merging requires two or more fragments to bind in overlapping regions and involves the design of molecules which incorporate motifs from each fragment.

In each case, designs are currently proposed on an ad hoc basis by human experts who draw on standard computational techniques and their deep understanding of chemistry to generate promising ideas. However, human experts may be hindered by implicit biases from past successes and failures, and when working with a large number of hits from a large fragment screen, it will not be feasible for a human expert to objectively assess all possible elaboration opportunities for suitability.

Recent years have seen significant interest in developing machine learning models to rapidly generate and screen large numbers of molecules as potential drug candidates. Different authors have employed a range of different molecular representations, including SMILES,[6] graphs,[7] SELFIES,[8] and atomic density grids,[9] and a number of different deep learning architectures, such as generative adversarial networks,[10] variational autoencoders[11] and recurrent neural networks.[12] With the aim of generating molecules with an optimal set of properties, several approaches have been proposed for multiobjective optimization, including gradient descent,[13] reinforcement learning,[12] Bayesian optimization[11] and particle swarm optimization.[14]

Received: October 29, 2021
Published: May 2, 2022

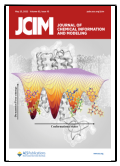

https://doi.org/10.1021/acs.jcim.1c01311
J. Chem. Inf. Model. 2022, 62, 2280−2292

While early generative models typically generated a molecule "from scratch", several authors have recently proposed deep learning-based methods to help improve the efficiency of fragment-to-lead campaigns. Graph-based approaches for scaffold elaboration were proposed by Lim et al.[15] and Li et al.,[16] which provide a model with a fragment and generate a set of molecules which contain the original fragment as a substructure, while Arús-Pous et al.[17] proposed a SMILES-based[18] model, Scaffold-Decorator, which gave the user the ability to decide which atoms in the fragment should be used as an exit vector, allowing greater control over the types of elaborations generated. However, none of the above approaches allow for the specification of a preferred elaboration size, which, combined with their inability to account for protein structure when generating elaborations, means they cannot ensure that elaborations made by the model would be of an appropriate size to fit within the binding pocket. More recently, we proposed DEVELOP,[19] a fragment-based generative model for linking and growing which built on our DeLinker[20] model. DEVELOP allows the specification of pharmacophoric constraints and linker/elaboration length, providing a greater degree of control over the resulting molecules. In concurrent work to DEVELOP, Fialková et al.[21] proposed LibINVENT, an extension to Scaffold-Decorator,[17] which can be used to design core-sharing chemical libraries using only specific chemical reactions. LibINVENT also allows users to generate molecules with high 3D similarity to an existing active molecule via reinforcement learning. However, both DEVELOP and LibINVENT are reliant on either a pre-existing active or human specification of pharmacophoric constraints to generate targeted sets of molecules, making them more suitable tools for R-group optimization than for designing compounds against a novel target.

Orthogonal to the generative approaches described above, several recent papers have proposed database-based approaches to compound design. A recent method, CReM,[22] is based on the idea that a fragment within the context of a larger molecule can be interchanged with another fragment that has been observed to have the same local context in another molecule. CReM identifies potential elaborations by searching a database of molecules for fragments which have the same local context as the specified exit vector. Other recent database-based approaches incorporate protein-specific information. FragRep[23] takes a protein and ligand as input and enumerates modifications to the ligand by cutting the ligand into fragments and replaces a fragment with similar fragments from a database which would preserve the same protein−ligand interactions, while DeepFrag[24] uses a structure-aware convolutional neural network to select the most appropriate elaborations from a database of possible elaborations.

For the task of generating molecules "from scratch", a number of authors have proposed generative models which extract information directly from the protein. Skalic et al.[25] used a GAN[26] to generate ligand shapes complementary to the binding pocket which were then used to generate potential molecules by employing a shape-captioning network. Masuda et al.[27] encoded atomic density grids into separate latent representations for ligands and proteins and trained a model to generate 3D ligand densities conditional on the protein structure, which were then translated into discrete molecular structures. While both papers demonstrated that the ligands generated by their respective models were dependent on the learned structural representations, the models do not facilitate the specification of a design hypothesis provided by a human expert. Kim et al.[28] used water pharmacophore models to learn the location of key protein pharmacophores which were then used to construct a training set of molecules with complementary pharmacophores. While this approach would more readily integrate into standard drug-discovery efforts, it requires the training of a separate deep learning model for every target, as each target requires a training set of compounds which match the water pharmacophores.

In this work, we propose STRIFE (**Str**ucture **I**nformed **F**ragment **E**laboration), a generative model for fragment elaboration which extracts interpretable and meaningful structural information from the protein and uses it to make elaborations. This is different to all existing fragment-based generative approaches which either extract information implicitly from known ligands or do not make use of any protein-specific information when generating molecules. To allow straightforward integration into fragment-to-lead campaigns, STRIFE is readily customizable; in addition to the design hypotheses extracted directly from the protein, we provide a simple-to-use functionality which allows users to specify their own design hypotheses and generate elaborations with the aim of satisfying a desired pharmacophore. In a large-scale evaluation derived from the CASF-2016 set,[29] we show that STRIFE offers substantial improvements over existing fragment-based models.[17,22] We further demonstrate the applicability of STRIFE to real-world FBDD campaigns through two fragment elaboration tasks derived from the literature. In the first, we make elaborations to a fragment bound to N-myristoyltransferase, a key component in rhinovirus assembly and infectivity, and show that STRIFE is able to generate several elaborations that are strikingly similar to a highly potent inhibitor.[30] To demonstrate how user-specified design hypotheses can be incorporated into STRIFE, we consider the fragment-inspired small molecule inhibitor of tumor necrosis factor reported by O'Connell et al.[31] In this example, the elaboration proposed by O'Connell et al.[31] induces a substantial movement in a Tyrosine side chain. We manually specified a design hypothesis to explore side-chain flexibility and successfully recovered the elaboration proposed by O'Connell et al.,[31] as well as a range of other elaborations which were predicted to induce a similar movement in the Tyrosine side chain.

METHODS

We present our deep generative model for fragment elaboration, STRIFE, which requires the user to specify a target protein, a bound fragment, and the fragment exit vector. In our previous work,[19] we demonstrated how the imposition of pharmacophoric constraints allowed a substantial degree of control over the types of functional groups added to a fragment. STRIFE builds on the approach proposed in Imrie et al.,[19] where the pharmacophoric constraints were extracted from existing active molecules by extracting pharmacophoric constraints directly from the protein, thereby extending its applicability to a much broader range of targets. Pharmacophoric information is extracted by calculating a fragment hotspot map[32] (FHM), which describes regions of the binding pocket that are likely to make a positive contribution to binding affinity. STRIFE then identifies pharmacophoric constraints which are likely to place a pharmacophore within a matching hotspot region and uses the pharmacophoric constraints to generate elaborations.

https://doi.org/10.1021/acs.jcim.1c01311
J. Chem. Inf. Model. 2022, 62, 2280−2292

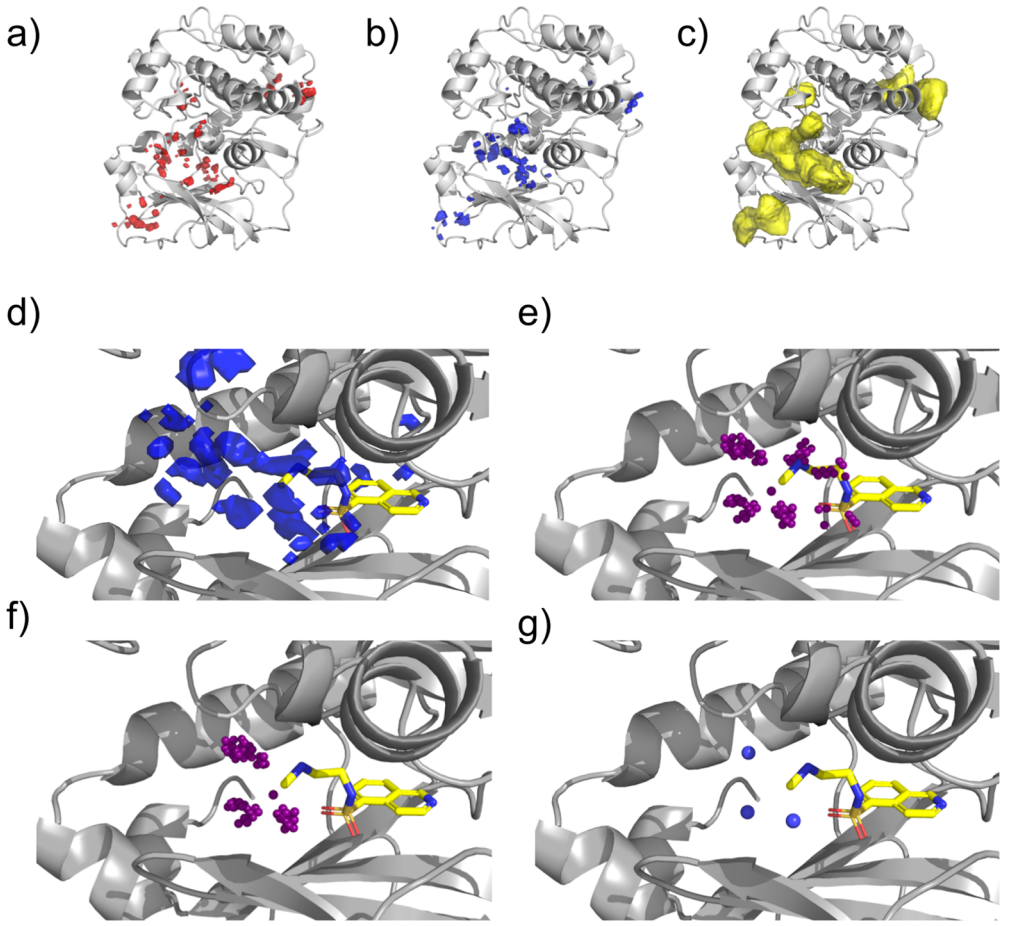

Figure 1. Processing fragment hotspot maps: (a) acceptor hotspot map, (b) donor hotspot map, and (c) apolar hotspot Map. A matching pharmacophore placed within a hotspot has a chance of making a disproportionate contribution to binding affinity. (d) An unprocessed donor hotspot map in the vicinity of the fragment of interest. (e) Each sphere represents a voxel in the hotspot map. Voxels which are too far away from the fragment exit vector are discarded. (f) Voxels which are closer to another fragment atom than the exit vector are removed. (g) Voxels are clustered based on their position. STRIFE attempts to generate elaborations such that a matching ligand pharmacophore is in close proximity to a cluster centroid.

Fragment Hotspot Maps. We calculate FHMs using the Hotspots API[33] which implements the algorithm described by Radoux et al.;[32] in this work, all FHMs were calculated using the default parameters given by Curran et al.[33] An FHM is calculated as follows: Atomic propensity maps are calculated using SuperStar,[34] which defines a grid covering the protein with equally spaced points 0.5 Å apart, and uses data from the Cambridge Structural Database (CSD)[35] to assign a propensity for a given probe type at each grid point. If an interaction between two groups at a certain distance and angle is particularly favorable, then it will occur more frequently in structures stored in the CSD and be assigned a higher propensity score. Once an atomic propensity map has been calculated, an FHM is derived by first weighting the scores assigned to each grid point in proportion to how buried in the protein the grid point is.

The FHM scores are then calculated by using small chemical probes which take the form of an aromatic ring with different atoms in the substituent position; for the apolar hotspot maps, the substituent is a methyl group, while for the acceptor and donor hotspot maps the substituent is a carbonyl and amine, respectively. The probes are translated to all grid points with weighted propensity scores above 15 and randomly rotated 3000 times about the center of the substituted atom. For each pose, each atom receives a score read from the weighted propensity map, and the probe scores are calculated as the geometric mean of the atom scores. As an atom receives a score of zero if it clashes with the protein, the geometric mean gives a score of 0 to any pose which clashes.

FHMs have a number of attractive properties. As only grid points with an above-threshold weighted propensity score are sampled, and the propensity scores are weighted by how buried in the protein they are, regions of the protein which are overly exposed are unlikely to be identified as hotspot regions. Additionally, because probe poses which clash with the protein attain a score of zero, any region identified as a fragment hotspot must be able to accommodate a molecule of reasonable size, meaning that the risk of attempting to satisfy a pharmacophore identified by the FHM which cannot be accessed by an elaboration is reduced.

FHM Processing. For a protein target, STRIFE uses FHMs to guide the generative model in the placement of functional groups which can interact with the target. As the different hotspot maps are used for different purposes, they are processed slightly differently (Figure 1): the acceptor and donor hotspots are used to identify desirable pharmacophoric constraints, while the apolar maps are used to verify that the fragment is located in an appropriate binding site. For the

https://doi.org/10.1021/acs.jcim.1c01311
J. Chem. Inf. Model. 2022, 62, 2280−2292

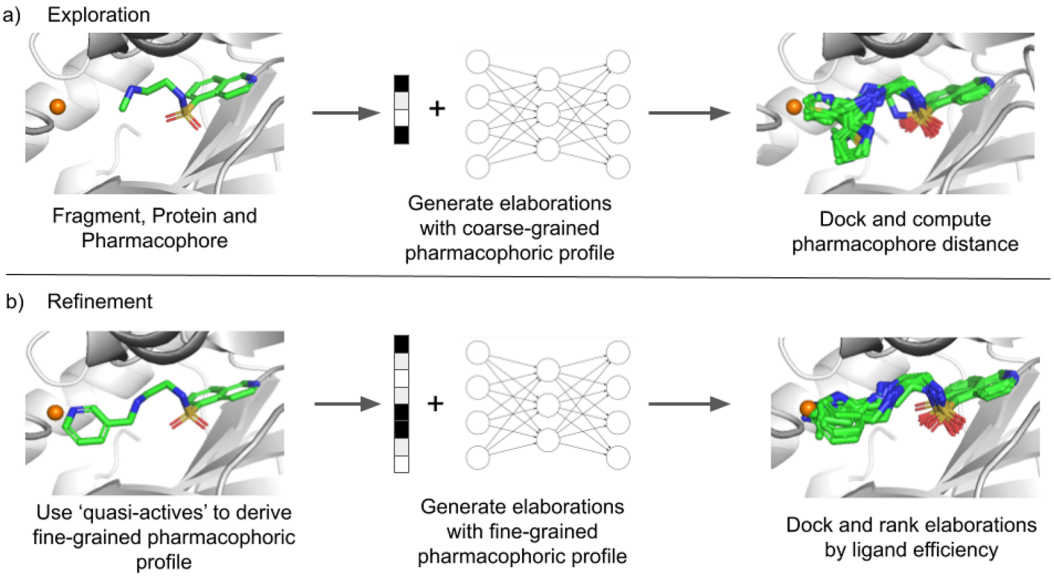

Figure 2. Illustration of how STRIFE generates elaborations which place pharmacophores close to a specified pharmacophoric point. (a) STRIFE first generates elaborations using a coarse-grained pharmacophoric profile and docks them using the constrained docking functionality in GOLD.[38] (b) Elaborations which placed a matching pharmacophore in close proximity to the pharmacophoric point are used to derive a fine-grained pharmacophoric profile. STRIFE then generates elaborations using those pharmacophoric profiles; the resulting molecules are docked and ranked by their predicted ligand efficiency.

apolar maps, we identify all grid points which have a value greater than 1 and discard all other points. Similarly, for the acceptor and donor maps, we retain all grid points which have a value greater than 10. While Radoux et al.[32] reported that values greater than 17 were generally predictive of fragment binding, we selected 10 as a threshold to obtain wider coverage; this parameter is simple to change to restrict the search to higher quality hotspots.

To process the acceptor and donor maps, all points which are less than 1.5 Å or greater than 5 Å from the fragment exit vector are discarded to allow for elaborations of appropriate length. These distance thresholds were chosen to reflect the iterative nature of a fragment-to-lead campaign, where practitioners typically make a succession of small elaborations, but they can be altered by the user to admit longer or shorter elaborations.

A greedy clustering algorithm is employed to identify contiguous hotspot regions as follows: A cluster is initialized as a single point and all unclustered points which are within 1 Å of the grid point are added to the cluster. For each point in the cluster, the distance to all remaining unclustered points is calculated, and any points which are within 1 Å are added to the cluster until no unclustered points can be added. Once a cluster has terminated, a new cluster is defined by selecting a single unclustered point until all points have been assigned to a cluster. For each hotspot cluster, centroids are defined by computing the mean position of the points in the cluster. To reduce redundancy, if two cluster centroids are closer than 1.5 Å apart, the cluster centroid corresponding to the smaller cluster is deleted. In addition, if a cluster is smaller than eight points, it is removed, unless no clusters of eight or more points exist, in which case smaller clusters are retained.

We use the apolar maps to conduct a final filtering step, adopting the heuristic that a molecule which is entirely contained within an apolar hotspot region has a better chance of binding to the protein. Therefore, if an acceptor or donor cluster centroid is not contained within a hotspot region, then it is filtered out. Additionally, if all fragment atoms are not contained within an apolar hotspot, then we consider the fragment to be unsuitable for elaboration and terminate the algorithm. While this might appear to be overly restrictive, in practice, the apolar hotspot maps typically cover the majority of binding sites in a target, and this filtering step can be easily negated if the user believes that a fragment is a suitable candidate for elaboration.

The final output of the processing scheme are the 3D coordinates of the remaining cluster centroids from the acceptor and donor maps (hereafter "pharmacophoric points"). In the subsequent molecule generation steps, our aim is to generate elaborations which place matching functional groups in close proximity to the pharmacophoric points. While the above pipeline automates the process of defining pharmacophoric points, we also provide a simple-to-use functionality for users to define their own pharmacophoric points, allowing them to pursue a range of different design hypotheses (see Methods and Customizability).

Next, we describe how STRIFE uses a set of pharmacophoric points to generate elaborations with complementary pharmacophores to the target.

Generative Model. The generative model employed by STRIFE is similar to our previous work, DEVELOP,[19] where the generative process is based upon the constrained graph variational autoencoder framework proposed by Liu et al.[7] STRIFE differs from DEVELOP in the structural information $\boldsymbol{D}$ provided to the model when decoding molecules (see Methods and STRIFE Algorithm). Given a fragment, $\boldsymbol{f}$, and structural information, $\boldsymbol{D}$, elaborations are generated as follows: Representing $\boldsymbol{f}$ as a graph, each node v is assigned an h-dimensional vector representation $\mathbf{z}_v$ and corresponding label l_v, denoting the atom type of the node. A set of K "expansion nodes", $\mathbf{z}_{v_1},\cdots,\mathbf{z}_{v_K}$ are generated by sampling from an h-dimensional standard normal distribution, and each expansion node is assigned a label l_{v_k} by a linear classifier which

https://doi.org/10.1021/acs.jcim.1c01311
J. Chem. Inf. Model. 2022, 62, 2280−2292

takes $\mathbf{z}_{v_k}$ and $\boldsymbol{D}$ as input. The expansion nodes represent the possible atoms which may be appended to the fragment.

Starting from the fragment exit vector, the model samples a node to add to the graph from the set of expansion nodes. To choose whether to form a bond between node v and node u, we use a neural network which takes as input

$$\phi_{v,u}^{t} = [t, s_v^t, s_u^t, d_{v,u}, \mathbf{H}^0, \mathbf{H}^t, \boldsymbol{D}]$$

where t is the number of time steps that have currently been taken. $s_v^t = [z_v^t, l_v]$ is the concatenation of latent vector and label at the tth time step. $d_{u,v}$ is the graph distance between u,v. H^j is the average of all latent vectors at the j^{th} time step.

After a new node has been added to the graph, a gated graph neural network[36] is used to update the encodings for each node to reflect its potentially altered neighborhood. This iterative approach continues until termination where the final molecule is returned. Additional details regarding the generative model framework can be found in our previous work.[19,20]

STRIFE Algorithm. Above, we described how STRIFE uses fragment hotspot maps (FHMs)[32] to obtain an interpretable representation of structural information and how, given a fragment, $\boldsymbol{f}$, and structural information, $\boldsymbol{D}$, we can generate elaborations to the fragment. Here, we describe how these processes fit within the STRIFE algorithm. In particular, we outline how the 3D pharmacophoric points derived from the FHMs are converted to a representation of structural information, $\boldsymbol{D}$, which is used to generate elaborations.

The structural information $\boldsymbol{D}$ can be provided to the generative model in two different forms. The first is a coarse-grained pharmacophoric representation, where the model is simply provided with a vector containing the number of hydrogen bond acceptors, the number of hydrogen bond donors, and the number of aromatic groups. The desired pharmacophoric profile of the generated elaborations can also be more precisely specified by adding the predicted path distances (the length of the shortest sequence of atoms connecting two points) from the exit vector to the pharmacophore, providing a greater degree of control over the types of elaborations made by the model. STRIFE utilizes both of these representations of pharmacophoric information at different stages of the algorithm. In the exploration phase (Figure 2a), STRIFE uses the coarse-grained representation to generate a wide range of elaborations, which are then assessed for suitability. In the refinement phase (Figure 2b), fine-grained pharmacophoric profiles are derived from the most suitable elaborations and are used to generate further elaborations. Additional details are provided below and in the Supporting Information.

In a standard fragment elaboration campaign, where practitioners typically work in an iterative way, making small elaborations to a fragment which is then optimized before making additional elaborations to the optimized molecule. In this paper, we demonstrate STRIFE-generating elaborations which place a pharmacophore close to a single pharmacophoric point at a time. For example, if the set of pharmacophoric points contains one donor and one acceptor, STRIFE will attempt to produce a set of elaborations which include a donor in close proximity to the donor pharmacophoric point and a set of elaborations which place an acceptor in close proximity to the acceptor pharmacophoric point but will not attempt to satisfy both pharmacophoric points simultaneously. STRIFE is capable of attempting to satisfy multiple pharmacophoric points simultaneously, but this is not recommended unless the pharmacophoric points have been manually specified or inspected by the user, as it may not be possible to simultaneously satisfy certain combinations of pharmacophores with a single elaboration. After obtaining a series of pharmacophoric points from the FHM, STRIFE proceeds as follows:

Exploration Phase. STRIFE aims to generate a set of elaborations which contain functional groups in close proximity to a pharmacophoric point. To facilitate this, for each pharmacophoric point, we predict the atom-length distance between the fragment exit vector and the pharmacophoric point using a trained support vector machine.[37] As the generative model requires the specification of a desired elaboration length, we use the atom-length prediction to control the length of elaborations proposed by STRIFE. To allow for the inclusion of rings and side chains in the elaboration, we use several different desired elaboration lengths; if the predicted atom distance is p, we generate elaborations with a requested length of up to $p + 4$. As well as specifying a desired elaboration size, the generative model requires us to specify a desired pharmacophoric profile. In the exploration phase, we generate molecules using the coarse-grained pharmacophoric profile; as the coarse-grained pharmacophoric profile does not specify a desired path distance between the exit vector and the ligand pharmacophore, the pharmacophores in the elaborations proposed by the generative model will occupy a broad range of different positions in the binding pocket.

The proposed elaborations are filtered (Supporting Information) and docked using the constrained docking functionality in GOLD,[38] where the structure of the fragment is provided as the constraint. Each molecule is docked 10 times, and the top-ranked pose selected. For each top-ranked pose, we compute the distance between the 3D pharmacophoric point and a matching pharmacophore in the molecule. We then identify all molecules where the resulting distance is less than 1.5 Å and select the five molecules for which the distance between pharmacophoric point and ligand pharmacophore is smallest. If less than five molecules exhibit a distance of less than 1.5 Å, we select only molecules which fulfill this criteria.

Refinement Phase. The molecules which exhibit a functional group in close proximity to a pharmacophoric point provide useful information, as they can be used to derive the more fine-grained representation of structural information which specifies the path distance between the exit vector and each ligand pharmacophore; as such, we refer to these molecules as "quasi-actives", because they play a similar role to known actives in existing generative models. Having obtained a set of quasi-actives for each pharmacophoric point and used them to derive a set of structural information vectors $\boldsymbol{D}_1, \boldsymbol{D}_2, \cdots, \boldsymbol{D}_n$, the user can either generate a fixed number of elaborations using each $\boldsymbol{D}_i$ or request a fixed total number of elaborations, where a structural information vector is randomly sampled from $\{\boldsymbol{D}_i\}_{i=1}^{n}$ for each elaboration. As before, the generated molecules are filtered and docked using the constrained docking functionality in GOLD.[38] Finally, each unique molecule, m, is ranked by its ligand efficiency, computed as the docking score divided by the number of heavy atoms, allowing the user to quickly prioritise a small number of elaborations for consideration.

https://doi.org/10.1021/acs.jcim.1c01311
J. Chem. Inf. Model. 2022, 62, 2280−2292

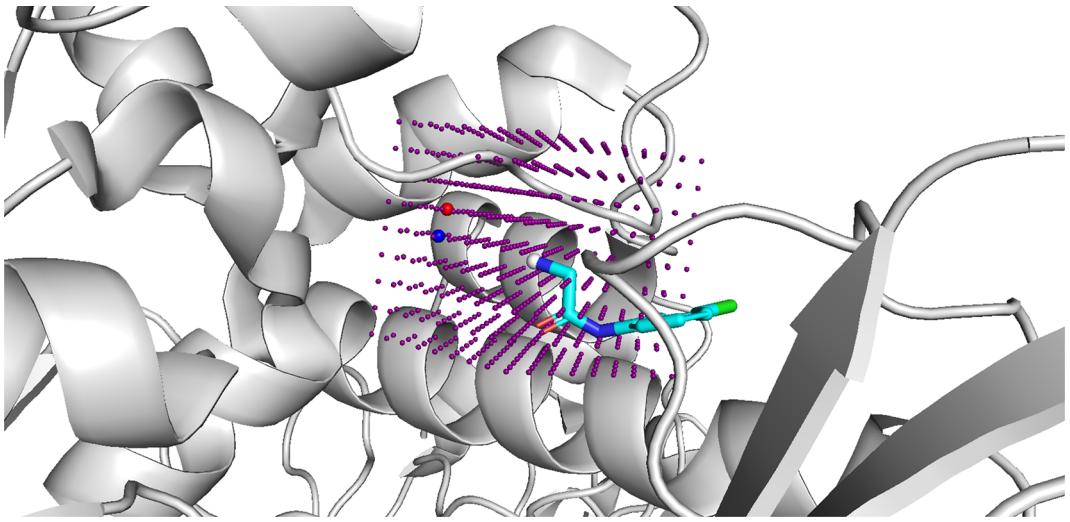

Figure 3. Example of how the pharmacophoric points provided to STRIFE can be customized using the molecule viewer PyMOL.[40] A lattice of points are centered about the fragment exit vector (denoted by the gray atom), and the user simply selects the point(s) they wish to denote as a pharmacophoric point and saves them in an SDF file. The red and blue points represent an acceptor point and donor point, respectively. STRIFE can then be run as usual and will attempt to make elaborations which places matching pharmacophores close to the user-specified pharmacophoric points.

ADMET Filtering. To reduce the likelihood of proposing molecules with undesirable ADMET characteristics, we provide an additional, optional filter that can be applied post hoc. The filter is based on the quantitative estimate of druglikeness (QED).[39] The QED score is based on a range of factors (e.g., hydrophobicity, molecular weight) which are important ADMET considerations, so can be used to quickly flag molecules which might exhibit problematic ADMET characteristics.

As the QED associated with an elaborated molecule will be heavily dependent on the original fragment, we use the QED attained by the original fragment as a threshold for flagging a molecule proposed by STRIFE. In other words, a molecule is flagged if it is predicted to be "less-druglike" than the original fragment. We also provide the option for the user to alter the flagging threshold.

Customizability. Although STRIFE can automatically extract a set of pharmacophoric points from a protein, in a real-world drug discovery setting, practitioners may wish to explore their own design hypotheses. To facilitate such usage, we provide a simple-to-use functionality which allows a user to manually specify the location of a pharmacophore in the context of the protein. The tool, shown in Figure 3, loads a lattice centered around the fragment exit vector into a molecule viewer. To manually specify their own pharmacophoric profiles, the user simply selects the lattice points corresponding to their desired pharmacophore location, saves the resulting object, and runs STRIFE as usual.

Model Training. We trained our generative models using a training set derived from the subset of ZINC[41] randomly selected by Gómez-Bombarelli et al.[6] For each molecule, we obtained a series of fragment−ligand pairs by enumerating all cuts of acyclic single bonds which were not part of functional groups. The resulting training set comprised approximately 427,000 examples. The same hyperparameters were used for training as in our previous work.[19]

Experiments. We assessed the ability of our model to make appropriate elaborations using a test set derived from the CASF-2016 set.[29] This test set was constructed using the same procedure used to generate our training set and initially comprised 237 examples. As our aim was to assess the ability of our model to learn from the structural information supplied by the FHMs, we excluded from our test sets examples where the ground truth molecule was not contained within an apolar hotspot region and examples where no suitable pharmacophoric points could be identified by the hotspots algorithm. In addition, we filtered examples where STRIFE was unable to identify any quasi-actives. These filtering steps removed 109, 26, and 1 examples from the test set, respectively, leaving a final test set of 101 examples (a full list is given in Table S1). While the filtering steps outlined above removed a substantial proportion of examples from our test set, the initial test set was constructed by fragmenting the ground truth ligand without consideration of the associated protein. As such, many of the fragments would not have been considered suitable candidates for elaboration.

Using the STRIFE pipeline (Figure 2), we sampled a set of 250 elaborations for each example in the test set. We compared STRIFE to four baselines: the deep generative model published by Arús-Pous et al.,[17] "Scaffold-Decorator", the database-based CReM and DeepFrag, and a truncated version of the STRIFE algorithm ($STRIFE_{NR}$) which generated elaborations from the coarse-grained model (essentially only conducting the exploration phase from Figure 2a and omitting the refinement phase). We provided CReM with the same set of 250,000 molecules we used to derive the training sets for STRIFE, which was converted into a database of fragments using CReM's fragmentation procedure. The Scaffold-Decorator model was trained using the same set of examples as the STRIFE generative models. For DeepFrag, we used the saved model trained by the original authors in the original publication;[24] as the DeepFrag training process requires a fragment and associated protein structure for each example, it is not possible to use the 250,000 subset of ZINC[41] to train the DeepFrag model. As DeepFrag is trained on an entirely separate region of chemical space compared to all other baselines, including protein−ligand complexes included in the CASF-2016 set, it is difficult to objectively compare it to the

https://doi.org/10.1021/acs.jcim.1c01311
J. Chem. Inf. Model. 2022, 62, 2280−2292

Table 1. Comparison of CReM, Scaffold-Decorator, DeepFrag, $STRIFE_{NR}$, and STRIFE on the CASF Test Set[a]

Metric	CReM	Scaffold-Decorator	DeepFrag	$STRIFE_{NR}$	STRIFE
Valid	**100%**	99.98%	**100%**	99.5%	98.96%
Unique	N/A	32.78%	N/A	**56.96%**	37.31%
Novel	N/A	4.23%	N/A	**55.65%**	49.21%
Pass 2D filters	66.06%	**98.2%**	78.47%	73.81%	75.38%
ΔQED	−0.148%	**-0.05%**	−0.125%	−0.09%	−0.086%
ΔSLE_{20}	−0.029	0.1	−0.177	0.44	**0.512**
ΔSLE_{50}	−0.489	−0.222	−0.56	0.078	**0.164**
ΔSLE_{100}	−0.992	−0.572	−0.979	−0.316	**-0.228**

[a]See Methods and Evaluation Metrics for definitions of the metrics. Bold indicates the best value obtained across the different methods.

other methods. We include the results from DeepFrag primarily for completeness to give an indication as to how STRIFE compares to another structure-aware approach.

Evaluation Metrics. For our experiments on the CASF test set, we report several standard 2D metrics in line with those reported in our previous work:[19]

- Validity: Proportion of generated molecules which could be parsed by RDKit[42] and for which at least one atom was added to the fragment.
- Uniqueness: Proportion of distinct molecules generated by the model, calculated as the number of distinct molecules divided by the total number of molecules.
- Novelty: Proportion of generated molecules for which the elaboration was not included in the model training set.
- Passed 2D Filters: Proportion of generated molecules which passed a set of 2D filters. A generated molecule was filtered out if the SAScore[43] of the generated molecule was higher (harder to synthesize) than the SAScore associated with the fragment, if the elaboration contained a nonaromatic ring with a double bond, or if the molecule failed to pass any of the pan-assay interference (PAINS)[44] filters.

We did not compute the proportion of unique or novel associations proposed by CReM, as CReM does not allow the specification of a desired number of elaborations. CReM returns the set of elaborations contained in the database deemed "reasonable", meaning that all elaborations proposed by CReM are by design unique. As CReM proposes molecules from a fixed vocabulary of possible elaborations, none of the elaborations proposed by CReM could be considered novel. Similarly, we did not compute novelty or uniqueness values for DeepFrag and for each example attributed 250 elaborations to DeepFrag by selecting the elaborations ranked 1−250 (from a vocabulary of 5000 possible elaborations) by DeepFrag's own ranking method.

In addition to the 2D metrics proposed above, we report an additional 2D metric based upon QED[39] to assess whether attempting to satisfy the identified pharmacophoric points impacts STRIFE's ability to generate druglike elaborations

- ΔQED: The average difference in the QED attained by the elaborated molecules and the original fragment, calculated as $\Delta QED = \frac{1}{n}\sum_{j=1}^{n}\Delta QED_j$, where $\Delta QED_j = \frac{1}{k}\sum_{i=1}^{k} QED(mol_{ij}) - QED(frag_j)$.

To assess the ability of STRIFE to generate elaborations capable of forming promising interactions with the target, we used the constrained docking functionality in GOLD[38] to dock each generated ligand 10 times and calculated the docking score of the top-ranked pose for each ligand. To mitigate the tendency of classical scoring functions to favor larger molecules over smaller ones,[45] we calculated the ligand efficiency of each molecule by dividing the docking score by the number of heavy atoms. To account for the variation in docking scores across different targets, we standardize the ligand efficiencies attained by a model on a specific example to have zero mean and unit variance, applying the same transformation to the ground truth ligand efficiency. For the jth example, we compute $\Delta SLE_{\alpha,j} = SLE_{\alpha,j} - SLE_{GT,j}$, where $SLE_{\alpha,j}$ is the average standardized ligand efficiency of the top α ranked molecules, and $SLE_{GT,j}$ is the standardized ligand efficiency of the corresponding ground truth. If α is specified as greater than the total number of elaborations for which the ligand efficiency was computed (as only molecules which pass the 2D filters are docked), we use the average standardized ligand efficiency of all such molecules. We average over all examples to obtain $\Delta SLE_\alpha = \frac{1}{n}\sum_{j=1}^{n}\Delta SLE_{\alpha,j}$. ΔSLE_α (standardized ligand efficiency improvement) only considers a subset of the molecules generated by each model, mirroring how a large number of molecules produced by a generative model would be assessed in a real-world fragment-to-lead campaign, where it is unlikely that a human expert would manually inspect hundreds of lowly ranked molecules.

As CReM is unable to return a fixed number of elaborations, we calculated three sets of summary statistics for CReM, each using a different subset of the test set. In all cases, if CReM returned more than 250 elaborations for a specific example, we sampled a set of 250 elaborations from the larger set:

- The set of examples for which CReM returned 250 elaborations (n = 45).
- The set of examples for which CReM returned 50 or more elaborations (n = 62).
- The set of examples for which CReM returned at least one elaboration (n = 82).

We present the results for the first set in Table 1 and compare the results between the three subsets in the Supporting Information (Table S2). In the case where we included all examples with at least one elaboration, the ΔSLE_α values were substantially degraded by the subset of examples where only a small number of elaborations were proposed.

RESULTS AND DISCUSSION

We assessed the ability of STRIFE to propose elaborations to fragments by incorporating meaningful pharmacophoric information into the generative process. Through a large scale evaluation on a test set derived from the CASF-2016

https://doi.org/10.1021/acs.jcim.1c01311
J. Chem. Inf. Model. 2022, 62, 2280−2292

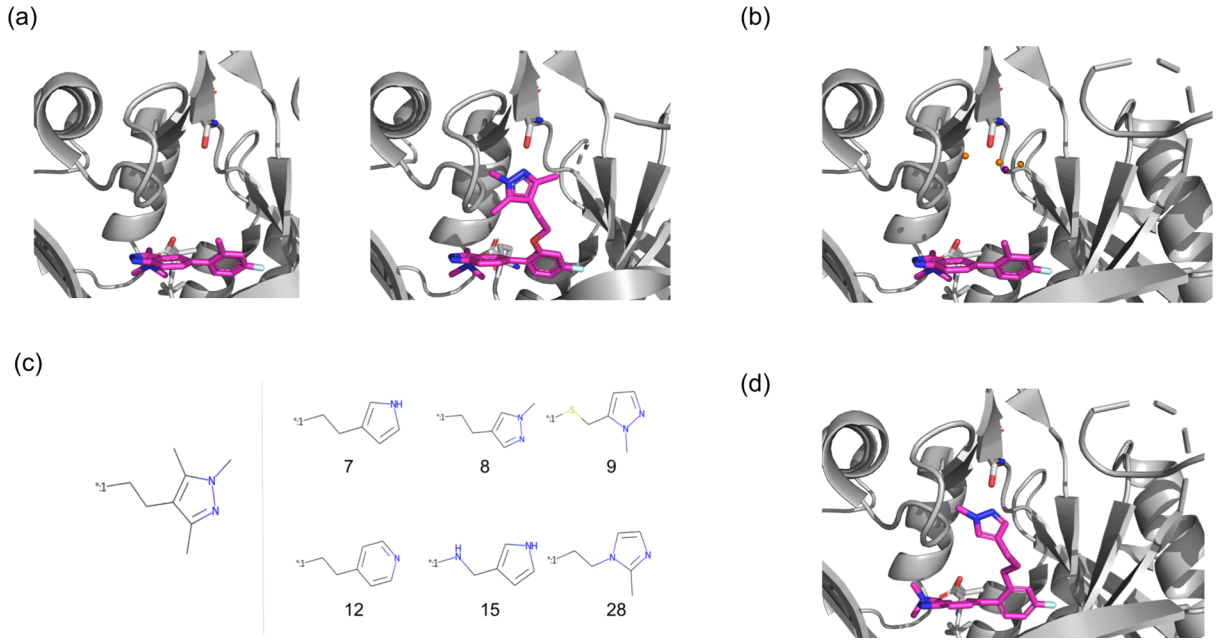

Figure 4. Fragment elaboration case study. (a) Left: Crystal structure (PDB ID: 5O48) of the fragment bound to *P. vivax* NMT. Right: Crystal structure (PDB ID: 5O6H) of the optimized compound bound to human NMT1. The trimethylpyralzole facilitates an interaction with the residue S319. (b) Processed pharmacophoric points from the fragment hotspot Map calculated on *P. vivax* NMT. The orange spheres correspond to hydrogen bond acceptor points, while the purple sphere corresponds to a hydrogen bond donor point. (c) Elaboration proposed by Mousnier et al.[30] (left) compared to several elaborations proposed by STRIFE which satisfied the same design hypothesis (right). The number underneath each elaboration corresponds to the rank assigned to it by STRIFE. (d) Docked pose of one of our elaborations, which appears to be capable of forming the same hydrogen bond interaction with S319.

set,[29] we show that STRIFE is able to generate a wide range of chemically valid elaborations, many of which were not contained in the training set. In addition, in terms of generating elaborations which exhibit high ligand efficiency, STRIFE substantially outperforms existing computational methods for fragment elaboration,[17,22] illustrating the advantages of incorporating structural information into the generative model. We demonstrate the applicability of STRIFE to real-world fragment-to-lead campaigns using two case studies derived from the literature; in particular, we show how STRIFE can be used to explore design hypotheses including side-chain movement.

Large Scale Experiments. Our experiments on the CASF set demonstrate the benefits of including structural information in the generative process (Table 1). All methods generated chemically valid elaborations in more than 99% of cases, illustrating their ability to apply basic valency rules. Scaffold-Decorator, the SMILES-based, structure-unaware generative model proposed by Arús-Pous et al.,[17] generated the smallest proportion of unique molecules (33%). $\text{STRIFE}_{\text{NR}}$, a truncated version of the STRIFE algorithm which terminates before the refinement phase so does not account for the location of fragment hotspots, generated a greater proportion of unique elaborations (57%) than STRIFE (37%). However, this is to be expected as the refinement phase of the algorithm attempts to sample elaborations from a greatly reduced chemical space compared to the exploration phase.

Illustrating its ability to generalize beyond the information provided in the training set, almost half (49%) of the elaborations proposed by STRIFE were not contained in the training set. By contrast, only 4% of the elaborations generated by Scaffold-Decorator were novel, suggesting that it relies more heavily on the training set when making elaborations. Almost all of the elaborations proposed by Scaffold-Decorator (98%) passed the set of 2D filters, compared to 75% of elaborations generated by STRIFE and 74% by $\text{STRIFE}_{\text{NR}}$. As nearly all of the elaborations proposed by Scaffold-Decorator were contained in the training set, which itself was filtered to remove undesirable elaborations, the high pass rate of 2D filters is unsurprising.

STRIFE obtained the second highest ΔQED value among the different methods, behind Scaffold-Decorator, suggesting that attempting to satisfy the pharmacophoric points extracted from the FHM did not unduly affect the ability of STRIFE to propose druglike elaborations. We note that on average, the molecules proposed by all methods were "less druglike" than the corresponding fragment. This is not entirely surprising as none of the models were trained to optimize the QED score, but all methods were able to produce a substantial number of elaborations that were more druglike than the original fragment (Table S3)

On ΔSLE, which assesses the ability of models to generate elaborations which are more ligand efficient than the ground truth ligand, models that incorporate structural information proposed more ligand efficient elaborations. When considering the top 20 elaborations, the elaborations generated by CReM ($\Delta\text{SLE}_{20} = -0.029$) and Scaffold-Decorator ($\Delta\text{SLE}_{20} = 0.1$) were on average less ligand efficient than the ground truth, in contrast to $\text{STRIFE}_{\text{NR}}$ ($\Delta\text{SLE}_{20} = 0.44$) and STRIFE ($\Delta\text{SLE}_{20} = 0.512$). These results indicate that the fine-grained pharmacophoric profiles extracted during the refinement phase allow STRIFE to generate more ligand efficient elaborations, as the model more often generates elaborations which place pharmacophores in close proximity to a pharmacophoric point. We observed the same trend when the top 50 and 100 elaborations were considered, although in

https://doi.org/10.1021/acs.jcim.1c01311
J. Chem. Inf. Model. 2022, 62, 2280−2292

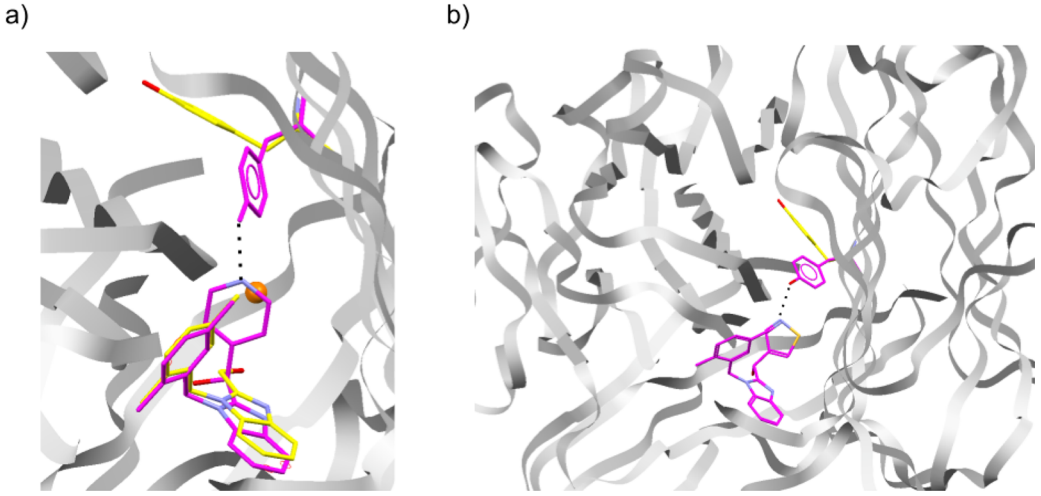

Figure 5. Visualization of flexible docking using Hermes[35] (a) fragment (yellow carbons, PDB ID: 6OOY) with elaborated molecule (magenta carbons, PDB ID: 6OOZ) reported by O'Connell et al.[31] The side chain of $Y119^{A}$ moved substantially to form a hydrogen bond. The orange sphere represents a user-specified pharmacophoric point which we provided as input to STRIFE. (b) An example of one of the molecules generated by STRIFE that appears to satisfy the specified design hypothesis. The molecule was docked into the fragment crystal structure (PDB ID: 6OOY, magenta side chain is the predicted conformation) using the flexible docking functionality in GOLD and supports the hypothesis that the side chain might move to accommodate the ligand.

this case the average ligand efficiency obtained by all models was lower than the ground truth ligand efficiency. We show how ΔSLE_{α} varies for different values of α in the Supporting Information (Figure S3).

In terms of the proportion of all generated elaborations which were more ligand efficient than the ground truth, STRIFE achieved the largest number, with 26% of elaborations obtaining a higher ligand efficiency than the ground truth, compared to 22%, 17%, and 12% for $STRIFE_{NR}$, Scaffold-Decorator, and CReM (when considering examples with 250 elaborations), respectively.

Comparison with DeepFrag. As mentioned above, it is difficult to objectively compare the performance of DeepFrag to the other baselines. As training examples for DeepFrag require a protein−fragment complex, DeepFrag may be hindered by the relatively scarcity of such structures (the Binding MOAD database[46] used to construct their training set contains approximately 40000 structures) and is therefore restricted to a much smaller region of chemical space compared to the other models. On the CASF test set, DeepFrag obtained the lowest ΔSLE_{20} and ΔSLE_{50} values across all models and only attained a better ΔSLE_{100} value than CReM. It is somewhat surprising that DeepFrag is not able to leverage the structural information provided to it to design more ligand efficient elaborations than the structure unaware Scaffold-Decorator; we provide additional information about the elaborations proposed by DeepFrag in the Supporting Information.

Fragment-Based Design of an N-Myristoyltransferase Inhibitor. Rhinovirus is a pathogen which plays a key role in complications arising in a variety of important respiratory diseases, including asthma, chronic obstructive pulmonary disease (COPD),[47] and cystic fibrosis.[48] Several studies[49,50] have reported that the host cell's N-myristoyltransferase (NMT) supports capsid assembly and infectivity, making NMT a potential antiviral drug target.

Following a fragment screen against NMT from the human malaria parasite *Plasmodium falciparum*,[51] Mousnier et al.[30] identified a fragmentlike compound, IMP-72 (Figure 4a), with weak (IC_{50} = 20 μM) activity against human NMT1 (HsNMT1). The binding mode of IMP-72 was originally determined in NMT from the malaria parasite *P. vivax* (PvNMT), but as the fragment's key interactions involved residues which are conserved in human NMTs, it was considered to be a viable starting point for the development of an HsNMT1 inhibitor. The authors noted that IMP-72 bound in a region complementary to a previously identified quinoline inhibitor,[52] MRT00057965; however, closer inspection of the overlaid binding modes precluded a fragment merging strategy. To address this, the authors constructed a simplified quinoline fragment, IMP-358, which could recapitulate the same interactions as MRT00057965 (S319 in PvNMT and S405 in HsNMT1) without clashing with IMP-72. Despite exhibiting weak inhibition of HsNMT1 (17% at a concentration of 100 μM), IMP-358 facilitated a synergistic inhibition alongside IMP-72, with the potency of IMP-72 increasing 300-fold for HsNMT1 in the presence of IMP-358. The authors developed a further compound, IMP-917, derived by replacing IMP-358 with a trimethylpyrazole group which was then linked to IMP-72 with an ether linker. Compared to IMP-72, IMP-917 exhibited a 1500-fold improvement in potency (IC_{50} = 0.013 μM) and retained the key interactions made by both IMP-72 and IMP-358. Finally, the authors made slight modifications to the core of IMP-917 and used the resulting compound to show that NMT inhibition completely prevents rhinoviral replication without inducing cytotoxicity, thereby identifying a potential drug target.

We investigated the ability of STRIFE to propose molecules that could satisfy the design hypothesis put forward by Mousnier et al.[30] Instead of iteratively refining the original quinoline fragment and constructing a linker, we viewed the task as an elaboration problem and sought to propose elaborations which could form interactions with S319. As input to STRIFE, we provided the SMILES string of IMP-72, the exit vector we wished to make elaborations from, and the crystal structure of PvNMT (PDB ID: 5O48). Although our aim was to design compounds for HsNMT1, we did not have access to a crystal structure of IMP-72 bound to HsNMT1, so

https://doi.org/10.1021/acs.jcim.1c01311
J. Chem. Inf. Model. 2022, 62, 2280−2292

given the high degree of conservation of NMTs across species, we considered it preferable to use the *P. vivax* NMT as opposed to docking IMP72 into the crystal structure of IMP-917 in complex with HsNMT1. We used STRIFE to generate 250 elaborations for IMP-72, which we docked using the constrained docking functionality in GOLD,[38] ranking each compound by its ligand efficiency. Figure 4C shows the structure added to IMP-72 to create IMP-917 and several highly ranked elaborations proposed by STRIFE which appear to be capable of interacting with the Serine residue in the same way. Despite only generating a total of 250 compounds, some of the molecules proposed by STRIFE bear a striking resemblance with the trimethylpyrazole elaboration proposed by Mousnier et al.[30] A list of all unique elaborations generated by STRIFE can be found in the Supporting Information (Figures S6−S10)

Customizability. While structure-aware generative models are increasingly being proposed, existing models incorporate such information through a single static structure, making them unable to account for the possibility that a side chain may move to interact with a ligand. By utilizing the flexible docking functionality in GOLD,[38] STRIFE allows the user to explore design hypotheses where a specified side chain moves; we illustrate how by considering a fragment-elaboration example from the literature.

O'Connell et al.[31] developed a small molecule inhibitor of tumor necrosis factor (TNF), a cytokine which has been shown to be a key factor in several autoimmune diseases, by making elaborations to a weakly binding fragment. The first elaboration allowed the formation of a hydrogen bond between the appended pyridyl group and the residue $Y119^A$, which moved substantially in order to make the interaction, yielding a 2500-fold improvement in binding affinity (Figure 5a).

The magnitude of the $Y119^A$ side-chain movement presents a challenge for a generative model, as it would not be possible for a structure-aware model to predict that the side chain would move, and if it was predicted by a chemist that the residue would be likely to move to form a hydrogen bond, then it would not be possible to communicate such information to the generative model. While STRIFE is unable to predict the movement of specific side chains in advance, if a human expert has reason to believe a side chain might move to accommodate a ligand, it is able to generate molecules which satisfy such a design hypothesis. This can be done by manually specifying a pharmacophoric point (see Methods and Customizability) such that a ligand pharmacophore placed at those coordinates would be able to interact with the residue side chain if it were to move in the hypothesized fashion. Under this setup, STRIFE attempts to generate molecules with pharmacophores close to the user-specified pharmacophoric point and uses the flexible docking functionality in GOLD[38] to dock the molecules while allowing the residue of interest to move freely; the user can then identify high scoring elaborations which were predicted to form the desired interaction with the protein.

To assess the ability of STRIFE to generate molecules which satisfied the design hypothesis specified by O'Connell et al.,[31] we manually specified a pharmacophoric point (Figure 5a) and generated 250 elaborations using the same procedure as for our other experiments. To allow GOLD's genetic algorithm to adequately explore the larger solution space created by side-chain flexibility, we generated 100 poses per molecule and used the highest scoring pose to calculate the corresponding ligand efficiency; further details of the flexible docking protocol can be found in the Supporting Information.

STRIFE successfully recovered the highly potent pyridyl elaboration proposed by O'Connell et al.,[31] while also proposing a wide range of structural analogues which appeared to be capable of making a similar hydrogen bond interaction with $Y119^A$. In particular, the most common elaboration proposed by the model was a pyridine with a meta substitution pattern. In total, 49 of the 250 elaborations contain a pyridine substructure, while 125 elaborations included a hydrogen bond acceptor that was also part of an aromatic group. Elaborations comprising a six-membered aromatic ring with a hydrogen bond acceptor were not scored among the most ligand efficient using GOLD's PLP scoring function, which generally rated pyrazole analogues or elaborations with hydrophobic groups more highly. However, consistent with the observed bound crystal structure, for both the ground truth pyridyl elaboration and several highly ranked elaborations which met the stated design hypothesis, the side chain of $Y119^A$ moved substantially to accommodate the proposed elaboration. An example is shown in Figure 5b, and further details of the elaborations proposed by STRIFE can be found in the Supporting Information (Figures S11 and S12).

The above analysis was dependent on manually choosing the location of the pharmacophoric point. To assess STRIFEs robustness to the exact positioning of the pharmacophoric point, we constructed a lattice of pharmacophoric points in the binding pocket (Figure S13) and used each one in turn as an input to STRIFE. As expected, modifying the position of the pharmacophoric point affected the types of elaborations proposed; pharmacophoric points that were placed closer to the fragment exit vector tended to produce shorter elaborations than when the pharmacophoric point was further away (Figure S14).

STRIFE successfully recovered the ground truth pyridyl elaboration for 11 of the 27 different pharmacophoric points, demonstrating its robustness to the exact placement of pharmacophoric points. However, it is of greater interest to assess how often STRIFE was able to generate elaborations with an equivalent pharmacophoric profile to the pyridyl ground truth, as such elaborations would likely have the best chance of exhibiting similar behavior to the pyridyl elaboration. For each pharmacophoric point in the lattice, we calculated the number of elaborations proposed by STRIFE which were of length 5 or 6 and contained an aromatic hydrogen bond acceptor and plotted the values against the distance between the fragment exit vector and pharmacophoric point (Figure S15). Figure S15 shows that when the pharmacophoric point was placed between 3 and 4 Å away from the exit vector, STRIFE was usually able to generate a sizable number of elaborations which had an equivalent pharmacophoric profile to the pyridyl ground truth. This suggests that STRIFE is fairly robust to the precise placement of the pharmacophoric point (it does not need to be placed in an exact spot in order to generate sensible elaborations) but also that the placement of the pharmacophoric point does strongly affect the elaborations produced.

In summary, despite only making a small number of elaborations, we were able to use the pharmacophoric information provided to make a range of plausible elaborations which satisfied the specified design hypothesis. In practice, predicting if and how a side chain may move is often extremely difficult, but in such cases, STRIFE can be used to assess the

https://doi.org/10.1021/acs.jcim.1c01311
J. Chem. Inf. Model. 2022, 62, 2280−2292

plausibility of such a movement and provide starting points for a fragment-to-lead campaign.

CONCLUSION

We have proposed a model for fragment elaboration which derives meaningful information from the target into the generative process; unlike other generative models for fragment elaboration, STRIFE can incorporate target-specific information without using an existing active (although information from existing actives can easily be incorporated).

Currently, STRIFE uses information from FHMs which guide the placement of hydrogen bond acceptors and donors within the appended structure. Although hydrogen bonds between ligands and proteins often lead to large improvements in binding affinity, they are by no means the only consideration when making elaborations to a fragment; the framework could easily be expanded to explicitly account for properties such as hydrophobicity and aromaticity, allowing a greater degree of control over the design process. While we have used FHMs to extract important information from the protein, one could also use alternative pharmacophore interaction fields, such as GRAILS[53] or T2F,[54] to extract similar information which could then be supplied to the generative model. A further limitation of the default implementation of STRIFE is that it does not seek to simultaneously satisfy multiple pharmacophoric points within a single elaboration, potentially curtailing its ability to generate highly efficient elaborations in some scenarios. However, fragment elaboration campaigns generally involve incrementally making small additions to the molecule, and STRIFE provides the functionality to attempt to simultaneously satisfy multiple pharmacophoric points (whether FHM derived or manually specified) should the user wish to.

While we have used a two stage exploration-and-refinement approach to generate the final set of molecules, using a coarse-grained pharmacophoric profile followed by a fine-grained one, an alternative approach would be to use a single stage where elaborations are generated using a large number of potential pharmacophoric profiles. However, we believe that our two-stage approach is likely to be more computationally efficient, as generating elaborations using a series of different fine-grained pharmacophoric profiles, without any assessment of the suitability of such profiles, would lead to docking large amounts of unsuitable molecules.

STRIFE ranks the final set of generated molecules by their predicted ligand efficiency, calculated by docking each molecule and dividing the docking score by the number of heavy atoms in the molecule. While docking scores are known to not correlate perfectly with experimental binding affinities (see, for example, ref 29), they have successfully been used in a variety of scenarios to quickly screen large libraries and prioritize small numbers of compounds for experimental validation[55−57] and can give a useful indication to a human expert over whether a molecule is likely to bind to the target. If a user wished to use an alternative metric to rank the molecules produced by STRIFE, they would easily be able to do so.

Compared to existing structure-unaware models for fragment elaboration, the STRIFE algorithm carries a moderate up-front computational cost in calculating an FHM and identifying the set of quasi-actives (between 30 and 60 min on a desktop computer, in most cases). However, the most significant computational expense when generating a large number of elaborations is the docking of each generated molecule to estimate its ligand efficiency. As the quasi-actives only need to be identified once for a given fragment, the computational cost associated with STRIFE is therefore broadly comparable to other methods when generating large sets of molecules.

Although STRIFE is capable of being applied with minimal user input, one area which requires user specification is the choice of fragment and the associated exit vector. In practice, screening a fragment library may reveal dozens of weakly binding hits, yielding a large set of fragment−exit vector pairs to be explored. STRIFE could readily sample exhaustively from each fragment and exit vector; however, a future avenue of research would be to develop a prioritization scheme capable of identifying promising starting points for a fragment-to-lead campaign to allow a more efficient allocation of resources.

An advantage of the representation of structural information that STRIFE extracts from the target is that it is extremely easy for a user to interpret. While this is useful in allowing the user to understand why STRIFE generates the kinds of elaborations it does for a specific target, it also allows the user to easily specify their own design hypotheses. As such, we hope that STRIFE will be useful both in cases where a practitioner wishes to automatically generate a set of elaborations to a fragment bound to a novel target and in cases where they wish to rapidly enumerate a set of elaborations that conforms to a specific design hypothesis and can be used as a basis for further designs.

DATA AND SOFTWARE AVAILABILITY

STRIFE is available to download at https://github.com/oxpig/STRIFE. The default implementation of STRIFE is dependent on the commercial CSD Python API for calculating FHMs and carrying out constrained docking with GOLD. Users without access to the CSD Python API can still use STRIFE by manually specifying pharmacophoric points (see Methods, Customizability) and using alternative docking software. SMILES strings of the molecules used to train the generative models and path length model can be accessed in the STRIFE github repository, as can the structures used for the large scale evaluation.

ASSOCIATED CONTENT

Supporting Information

The Supporting Information is available free of charge at https://pubs.acs.org/doi/10.1021/acs.jcim.1c01311.

> Additional details of STRIFE algorithm, list of all ligands and proteins used in the CASF test set, additional results using CReM algorithm, performance of different methods on ΔSLE_α for different values of α, proportion of molecules generated with a higher QED than the starting fragment, details of molecules proposed by STRIFE and DeepFrag, and flexible docking protocol for case study (PDF)

AUTHOR INFORMATION

Corresponding Author

Charlotte M. Deane − *Oxford Protein Informatics Group, Department of Statistics, University of Oxford, Oxford OX1 3LB, United Kingdom;* orcid.org/0000-0003-1388-2252; Email: deane@stats.ox.ac.uk

https://doi.org/10.1021/acs.jcim.1c01311
J. Chem. Inf. Model. 2022, 62, 2280−2292

Authors

Thomas E. Hadfield − *Oxford Protein Informatics Group, Department of Statistics, University of Oxford, Oxford OX1 3LB, United Kingdom;* orcid.org/0000-0001-5397-6320

Fergus Imrie − *Oxford Protein Informatics Group, Department of Statistics, University of Oxford, Oxford OX1 3LB, United Kingdom;* orcid.org/0000-0002-6241-0123

Andy Merritt − *LifeArc, Stevenage SG1 2FX, United Kingdom;* orcid.org/0000-0002-0787-1648

Kristian Birchall − *LifeArc, Stevenage SG1 2FX, United Kingdom*

Complete contact information is available at: https://pubs.acs.org/10.1021/acs.jcim.1c01311

Notes

The authors declare no competing financial interest.

■ ACKNOWLEDGMENTS

T.E.H. is supported by funding from the Engineering and Physical Sciences Research Council (EPSRC), LifeArc, F. Hoffmann-La Roche AG, and UCB Pharma (Reference: EP/L016044/1). F.I. is supported by funding from EPSRC and Exscientia (Reference: EP/N509711/1). The authors would like to thank Mihaela Smilova, Ruben Sanchez-Garcia, Torsten Schindler, Lewis Vidler, Will Pitt, Vladas Oleinikovas, and Garrett M. Morris for helpful discussions.

■ REFERENCES

(1) Zhang, C.; Ibrahim, P. N.; Zhang, J.; Burton, E. A.; Habets, G.; Zhang, Y.; Powell, B.; West, B. L.; Matusow, B.; Tsang, G.; Shellooe, R.; Carias, H.; Nguyen, H.; Marimuthu, A.; Zhang, K. Y. J.; Oh, A.; Bremer, R.; Hurt, C. R.; Artis, D. R.; Wu, G.; Nespi, M.; Spevak, W.; Lin, P.; Nolop, K.; Hirth, P.; Tesch, G. H.; Bollag, G. Design and Pharmacology of a Highly Specific Dual FMS and KIT Kinase Inhibitor. *P. Natl. Acad. Sci.* **2013**, *110*, 5689−5694.

(2) Murray, C. W.; Newell, D. R.; Angibaud, P. A Successful Collaboration between Academia, Biotech and Pharma Led to Discovery of Erdafitinib, A Selective FGFR Inhibitor Recently Approved by the FDA. *MedChemComm* **2019**, *10*, 1509−1511.

(3) Murray, C. W.; Rees, D. C. The Rise of Fragment-Based Drug Discovery. *Nat. Chem.* **2009**, *1*, 187−192.

(4) Schuffenhauer, A.; Ruedisser, S.; Marzinzik, A.; Jahnke, W.; Selzer, P.; Jacoby, E. Library Design for Fragment Based Screening. *Curr. Top. Med. Chem.* **2005**, *5*, 751−762.

(5) Lamoree, B.; Hubbard, R. E. Current Perspectives in Fragment-Based Lead Discovery (FBLD). *Essays Biochem* **2017**, *61*, 453−464.

(6) Gómez-Bombarelli, R.; Wei, J. N.; Duvenaud, D.; Hernández-Lobato, J. M.; Sánchez-Lengeling, B.; Sheberla, D.; Aguilera-Iparraguirre, J.; Hirzel, T. D.; Adams, R. P.; Aspuru-Guzik, A. Automatic Chemical Design Using a Data-Driven Continuous Representation of Molecules. *ACS Cent. Sci.* **2018**, *4*, 268−276.

(7) Liu, Q.; Allamanis, M.; Brockschmidt, M.; Gaunt, A. L. Constrained Graph Variational Autoencoders for Molecule Design. *arXiv Preprint*, arXiv:1805.09076, 2018.

(8) Krenn, M.; Häse, F.; Nigam, A.; Friederich, P.; Aspuru-Guzik, A. Self-Referencing Embedded Strings (SELFIES): A 100% Robust Molecular String Representation. *Mach. Learn. Sci. Technol.* **2020**, *1*, No. 045024.

(9) Ragoza, M. T.; Masuda, T.; Koes, D. R. Generating 3D Molecules Conditional on Receptor Binding Sites with Deep Generative Models. *Chem. Sci.* **2022**, *13*, 2701.

(10) Guimaraes, G. L.; Sanchez-Lengeling, B.; Outeiral, C.; Farias, P. L. C.; Aspuru-Guzik, A. Objective-Reinforced Generative Adversarial Networks (ORGAN) for Sequence Generation Models. *arXiv Preprint*, arXiv:1705.10843, 2017.

(11) Jin, W.; Barzilay, R.; Jaakkola, T. Junction Tree Variational Autoencoder for Molecular Graph Generation. *Proceedings of the 35th International Conference on Machine Learning*, Stockholm, Sweden, PMLR 80, 2018; pp 2323−2332.

(12) Olivecrona, M.; Blaschke, T.; Engkvist, O.; Chen, H. Molecular De-Novo Design through Deep Reinforcement Learning. *J. Cheminf.* **2017**, *9*, 1−14.

(13) Gao, K.; Nguyen, D. D.; Tu, M.; Wei, G.-W. Generative Network Complex for the Automated Generation of Drug-Like Molecules. *J. Chem. Inf. Model.* **2020**, *60*, 5682−5698.

(14) Winter, R.; Montanari, F.; Steffen, A.; Briem, H.; Noé, F.; Clevert, D.-A. Efficient Multi-Objective Molecular Optimization in a Continuous Latent Space. *Chem. Sci.* **2019**, *10*, 8016−8024.

(15) Lim, J.; Hwang, S.-Y.; Moon, S.; Kim, S.; Kim, W. Y. Scaffold-Based Molecular Design with a Graph Generative Model. *Chem. Sci.* **2020**, *11*, 1153−1164.

(16) Li, Y.; Hu, J.; Wang, Y.; Zhou, J.; Zhang, L.; Liu, Z. Deepscaffold: A Comprehensive Tool for Scaffold-Based De Novo Drug Discovery Using Deep Learning. *J. Chem. Inf. Model.* **2020**, *60*, 77−91.

(17) Arús-Pous, J.; Patronov, A.; Bjerrum, E. J.; Tyrchan, C.; Reymond, J.-L.; Chen, H.; Engkvist, O. SMILES-Based Deep Generative Scaffold Decorator for De-Novo Drug Design. *J. Cheminf.* **2020**, *12*, 38.

(18) Weininger, D. SMILES, A Chemical Language and Information System. 1. Introduction to Methodology and Encoding Rules. *J. Chem. Inf. Comp. Sci.* **1988**, *28*, 31−36.

(19) Imrie, F.; Hadfield, T. E.; Bradley, A. R.; Deane, C. M. Deep Generative Design with 3D Pharmacophoric Constraints. *Chem. Sci.* **2021**, *12*, 14577−14589.

(20) Imrie, F.; Bradley, A. R.; van der Schaar, M.; Deane, C. M. Deep Generative Models for 3d Linker Design. *J. Chem. Inf. Model.* **2020**, *60*, 1983−1995.

(21) Fialková, V.; Zhao, J.; Papadopoulos, K.; Engkvist, O.; Bjerrum, E. J.; Kogej, T.; Patronov, A. LibINVENT: Reaction-Based Generative Scaffold Decoration for In Silico Library Design. *J. Chem. Inf. Model.* **2021**, DOI: 10.1021/acs.jcim.1c00469.

(22) Polishchuk, P. CReM: Chemically Reasonable Mutations Framework for Structure Generation. *J. Cheminf.* **2020**, *12*, 1−18.

(23) Shan, J.; Pan, X.; Wang, X.; Xiao, X.; Ji, C. FragRep: A Web Server for Structure-Based Drug Design by Fragment Replacement. *J. Chem. Inf. Model.* **2020**, *60*, 5900−5906.

(24) Green, H.; Koes, D. R.; Durrant, J. D. DeepFrag: A Deep Convolutional Neural Network For Fragment-Based Lead Optimization. *Chem. Sci.* **2021**, *12*, 8036.

(25) Skalic, M.; Sabbadin, D.; Sattarov, B.; Sciabola, S.; De Fabritiis, G. From Target to Drug: Generative Modeling for the Multimodal Structure-Based Ligand Design. *Mol. Pharmaceutics* **2019**, *16*, 4282−4291.

(26) Goodfellow, I.; Pouget-Abadie, J.; Mirza, M.; Xu, B.; Warde-Farley, D.; Ozair, S.; Courville, A.; Bengio, Y. Generative Adversarial Nets. *Advances in Neural Information Processing Systems 27*, 2014.

(27) Masuda, T.; Ragoza, M.; Koes, D. R. Generating 3D Molecular Structures Conditional on a Receptor Binding Site with Deep Generative Models. *arXiv Preprint*, arXiv:2010.14442, 2020.

(28) Kim, M.; Park, K.; Kim, W.; Jung, S.; Cho, A. E. Target-Specific Drug Design Method Combining Deep Learning and Water Pharmacophore. *J. Chem. Inf. Model.* **2021**, *61*, 36−45.

(29) Su, M.; Yang, Q.; Du, Y.; Feng, G.; Liu, Z.; Li, Y.; Wang, R. Comparative Assessment of Scoring Functions: The CASF-2016 Update. *J. Chem. Inf. Model.* **2019**, *59*, 895−913.

(30) Mousnier, A.; Bell, A. S.; Swieboda, D. P.; Morales-Sanfrutos, J.; Pérez-Dorado, I.; Brannigan, J. A.; Newman, J.; Ritzefeld, M.; Hutton, J. A.; Guedán, A.; Asfor, A. S.; Robinson, S. W.; Hopkins-Navratilova, I.; Wilkinson, A. J.; Johnston, S. L.; Leatherbarrow, R. J.; Tuthill, T. J.; Solari, R.; Tate, E. W. Fragment-Derived Inhibitors of Human N-Myristoyltransferase Block Capsid Assembly and Replication of the Common Cold Virus. *Nat. Chem.* **2018**, *10*, 599−606.

(31) O'Connell, J.; Porter, J.; Kroeplien, B.; Norman, T.; Rapecki, S.; Davis, R.; McMillan, D.; Arakaki, T.; Burgin, A.; Fox III, D.; Ceska, T.; Lecomte, F.; Maloney, A.; Vugler, A.; Carrington, B.; Cossins, B. P; Bourne, T.; Lawson, A. Small Molecules That Inhibit TNF Signalling By Stabilising An Asymmetric Form Of The Trimer. *Nat. Comms.* **2019**, *10*, 1−12.
(32) Radoux, C. J.; Olsson, T. S.; Pitt, W. R.; Groom, C. R.; Blundell, T. L. Identifying Interactions That Determine Fragment Binding at Protein Hotspots. *J. Med. Chem.* **2016**, *59*, 4314−4325.
(33) Curran, P. R.; Radoux, C. J.; Smilova, M. D.; Sykes, R. A.; Higueruelo, A. P.; Bradley, A. R.; Marsden, B. D.; Spring, D. R.; Blundell, T. L.; Leach, A. R.; Pitt, W. R.; Cole, J. C. Hotspots API: A Python Package for the Detection Of Small Molecule Binding Hotspots and Application to Structure-Based Drug Design. *J. Chem. Inf. Model.* **2020**, *60*, 1911−1916.
(34) Verdonk, M. L.; Cole, J. C.; Taylor, R. SuperStar: A Knowledge-Based Approach for Identifying Interaction Sites in Proteins. *J. Mol. Biol.* **1999**, *289*, 1093−1108.
(35) Groom, C. R.; Bruno, I. J.; Lightfoot, M. P.; Ward, S. C. The Cambridge Structural Database. *Acta Crystallogr. B* **2016**, *72*, 171−179.
(36) Li, Y.; Tarlow, D.; Brockschmidt, M.; Zemel, R. Gated Graph Sequence Neural Networks. *arXiv Preprint*, arXiv:1511.05493, 2015.
(37) Cortes, C.; Vapnik, V. Support-Vector Networks. *Mach. Learn.* **1995**, *20*, 273−297.
(38) Verdonk, M. L.; Cole, J. C.; Hartshorn, M. J.; Murray, C. W.; Taylor, R. D. Improved Protein−Ligand Docking Using GOLD. *Proteins* **2003**, *52*, 609−623.
(39) Bickerton, G. R.; Paolini, G. V.; Besnard, J.; Muresan, S.; Hopkins, A. L. Quantifying the Chemical Beauty of Drugs. *Nat. Chem.* **2012**, *4*, 90−98.
(40) Schrödinger, LLC; *The PyMOL Molecular Graphics System, Version 2.5*, 2010.
(41) Sterling, T.; Irwin, J. J. ZINC 15−Ligand Discovery for Everyone. *J. Chem. Inf. Model.* **2015**, *55*, 2324−2337.
(42) Landrum, G. RDKit: Open-Source Cheminformatics, 2006.
(43) Ertl, P.; Schuffenhauer, A. Estimation of Synthetic Accessibility Score of Drug-Like Molecules Based on Molecular Complexity and Fragment Contributions. *J. Cheminf.* **2009**, *1*, 1−11.
(44) Baell, J. B.; Holloway, G. A. New Substructure Filters for Removal of Pan Assay Interference Compounds (PAINS) from Screening Libraries and for Their Exclusion In Bioassays. *J. Med. Chem.* **2010**, *53*, 2719−2740.
(45) Boittier, E. D.; Tang, Y. Y.; Buckley, M. E.; Schuurs, Z. P.; Richard, D. J.; Gandhi, N. S. Assessing Molecular Docking Tools to Guide Targeted Drug Discovery of CD38 Inhibitors. *Int. J. Mol. Sci.* **2020**, *21*, 5183.
(46) Smith, R. D.; Clark, J. J.; Ahmed, A.; Orban, Z. J.; Dunbar, J. B., Jr; Carlson, H. A. Updates to Binding MOAD (Mother of All Databases): Polypharmacology Tools and Their Utility in Drug Repurposing. *J. Mol. Biol.* **2019**, *431*, 2423−2433.
(47) Ritchie, A. I.; Farne, H. A.; Singanayagam, A.; Jackson, D. J.; Mallia, P.; Johnston, S. L. Pathogenesis of Viral Infection in Exacerbations of Airway Disease. *Ann. Am. Thorac. Soc.* **2015**, *12*, S115−S132.
(48) Kieninger, E.; Singer, F.; Tapparel, C.; Alves, M. P.; Latzin, P.; Tan, H.-L.; Bossley, C.; Casaulta, C.; Bush, A.; Davies, J. C.; Kaiser, L.; Regamey, N. High Rhinovirus Burden in Lower Airways of Children with Cystic Fibrosis. *Chest* **2013**, *143*, 782−790.
(49) Marc, D.; Drugeon, G.; Haenni, A.-L.; Girard, M.; van der Werf, S. Role of Myristoylation of Poliovirus Capsid Protein VP4 as Determined by Site-Directed Mutagenesis of Its N-terminal Sequence. *EMBO journal* **1989**, *8*, 2661−2668.
(50) Marc, D.; Masson, G.; Girard, M.; van der Werf, S. Lack of Myristoylation of Poliovirus Capsid Polypeptide VP0 Prevents The Formation of Virions or Results in the Assembly of Noninfectious Virus Particles. *J. Virol.* **1990**, *64*, 4099−4107.
(51) Bell, A. S.; Mills, J. E.; Williams, G. P.; Brannigan, J. A.; Wilkinson, A. J.; Parkinson, T.; Leatherbarrow, R. J.; Tate, E. W.; Holder, A. A.; Smith, D. F. Selective Inhibitors of Protozoan Protein N-myristoyltransferases as Starting Points for Tropical Disease Medicinal Chemistry Programs. *PLoS Negl Trop Dis* **2012**, *6*, No. e1625.
(52) Goncalves, V.; Brannigan, J. A.; Whalley, D.; Ansell, K. H.; Saxty, B.; Holder, A. A.; Wilkinson, A. J.; Tate, E. W.; Leatherbarrow, R. J. Discovery of Plasmodium Vivax N-Myristoyltransferase Inhibitors: Screening, Synthesis, and Structural Characterization of Their Binding Mode. *J. Med. Chem.* **2012**, *55*, 3578−3582.
(53) Schuetz, D. A.; Seidel, T.; Garon, A.; Martini, R.; Korbel, M.; Ecker, G. F.; Langer, T. GRAIL: Grids of Pharmacophore Interaction Fields. *J. Chem. Theory Comput.* **2018**, *14*, 4958−4970.
(54) Mortier, J.; Dhakal, P.; Volkamer, A. Truly Target-Focused Pharmacophore Modeling: A Novel Tool for Mapping Intermolecular Surfaces. *Molecules* **2018**, *23*, 1959.
(55) Stein, R. M.; Kang, H. J.; McCorvy, J. D.; Glatfelter, G. C.; Jones, A. J.; Che, T.; Slocum, S.; Huang, X.-P.; Savych, O.; Moroz, Y. S.; et al. Virtual Discovery of Melatonin Receptor Ligands to Modulate Circadian Rhythms. *Nature* **2020**, *579*, 609−614.
(56) Lyu, J.; Wang, S.; Balius, T. E.; Singh, I.; Levit, A.; Moroz, Y. S.; O'Meara, M. J.; Che, T.; Algaa, E.; Tolmachova, K.; Tolmachev, A. A.; Shoichet, B. K.; Roth, B. L.; Irwin, J. J. Ultra-Large Library Docking for Discovering New Chemotypes. *Nature* **2019**, *566*, 224−229.
(57) Gorgulla, C.; Boeszoermenyi, A.; Wang, Z.-F.; Fischer, P. D.; Coote, P. W.; Padmanabha Das, K. M.; Malets, Y. S.; Radchenko, D. S.; Moroz, Y. S.; Scott, D. A.; Fackeldey, K.; Hoffmann, M.; Iavniuk, I.; Wagner, G.; Arthanari, H. An Open-Source Drug Discovery Platform Enables Ultra-Large Virtual Screens. *Nature* **2020**, *580*, 663−668.

https://doi.org/10.1021/acs.jcim.1c01311
J. Chem. Inf. Model. 2022, 62, 2280−2292